Structure Adaptation in Stochastic Inverse Methods for Integrating Information

**Carlos Llopis-Albert · José M. Merigó ·
Daniel Palacios-Marqués**

Abstract The use of inverse modeling techniques has greatly increased during the past several years because the advances in numerical modeling and increased computing power. Most of these methods require an a priori definition of the stochastic structure of conductivity (K) fields that is inferred only from K measurements. Therefore, the additional conditioning data, that implicitly integrate information not captured by K data, might lead to changes in the a priori model. Different inverse methods allow different degrees of structure adaptation to the whole set of data during the conditioning procedure. This paper illustrates the application of a powerful stochastic inverse method, the Gradual Conditioning (GC) method, to two different sets of data, both non-multiGaussian. One is based on a 2D synthetic aquifer and another on a real-complex case study, the Macrodispersion Experiment (MADE-2), site on Columbus Air Force Base in Mississippi (USA). We have analyzed how additional data change the a priori model on account of the perturbations performed when constraining stochastic simulations to data. Results show how the GC method tends to honour the a priori model in the synthetic case, showing fluctuations around it for the different simulated fields. However, in the 3D real case study, it is shown how the a priori structure is slightly modified not obeying just to fluctuations but possibly to the effect of the additional information on K, implicit in piezometric and concentration data. We conclude that implementing inversion methods able to yield a posteriori structure that incorporate more data might be of great importance in real cases in order to reduce uncertainty and to deal with risk assessment projects.

Keywords Stochastic inversion · Gradual deformation · Mass transport · Secondary data · Non-Gaussian

C. Llopis-Albert (✉)
Instituto Geológico y Minero de España (IGME), C/Cirilo Amorós, 42 – Entreplanta, 46004 Valencia, Spain
e-mail: cllopisa@gmail.com

J. M. Merigó
University of Manchester, Booth Street West, M15 6PB Manchester, UK
e-mail: jose.merigolindahl@mbs.ac.uk

D. Palacios-Marqués
Universitat Politècnica de València, Camí de Vera s/n, València, Spain 46022
e-mail: dapamar@doe.upv.es

1 Introduction

Numerical modeling of groundwater flow and mass transport has received considerable attention nowadays because it has become a reference criterion for water resources assessment and environmental protection. In this sense, there exists a high level awareness of the need for accurately characterize the heterogeneity in flow and mass transport models in order to provide reliable future predictions. In hydrogeology, inverse modeling is used to reduce the uncertainty by integrating data to better characterize the spatial variability of hydrogeologic properties. The knowledge that hydraulic conductivity (K) in soils and rocks is usually the parameter with the most significant spatial variation, with possible variations of several orders of magnitude within a short distance (Rehfeldt et al. 1992; Salamon et al. 2007; Llopis-Albert and Capilla 2009a, 2010a), triggered the development of highly sophisticated approaches to characterize these processes. Several comprehensive reviews of these inverse methods were presented by different authors (Yeh 1986; McLaughlin and Townley 1996; Zimmerman et al. 1998;; De Marsily et al. 2000; Carrera et al. 2005; Oliver and Chen 2010; Zhou et al. 2014). In addition, the most used codes for parameter estimation, sensitivity analyses and uncertainty analysis are PEST (Doherty 1994), UCODE (Poeter and Hill 1998) and the Generalized Likelihood Uncertainty Estimation, GLUE (e.g., Vázquez et al. 2009).

Many inverse problems are ill-posed in the sense that multiple solutions can be found that match the data. To impose constraints on those solutions, a prior distribution of the model parameters is required. In a spatial context, the a priori structure can be as simple as a Multi-Gaussian law with prior covariance matrix, or be presented in the form of a complex training image describing the prior statistics of the model parameters (Caers 2007).

Therefore, most of the inverse methods require an a priori definition of the stochastic structure of K fields that is inferred only from K measurements. Thus, the additional conditioning data, that implicitly integrate information not captured by K data, is not taken into account. The different inverse methods available in the literature allow different degrees of structure adaptation to the whole set of data during the conditioning procedure.

This paper shows the worth of implementing inversion methods able to yield a posteriori structures, that incorporate as much data as possible, in order to provide reliable predictions and to reduce uncertainty.

Among the large number of inverse modelling techniques available in the literature, the Gradual Conditioning (GC) method is used because of its powerful capabilities as explained in the next section (Capilla and Llopis-Albert 2009; Llopis-Albert and Capilla 2009a, 2009b, 2010a; 2010b; 2011). This stochastic inverse method belongs to the category of those methods developed to generate conditional simulations to assess model uncertainties through the analysis of multiple equally likely realizations, e.g., Gómez-Hernández et al. (1997). In the GC method, the priori stochastic structure is inferred from K data, secondary data and by the corresponding indicator variograms. Then the changes of the a priori structure (i.e., the perturbations when constraining stochastic simulations to data) are performed by means of the ccdf's and the probabilities fields (Capilla and Llopis-Albert 2009). As a result, the additional data change the a priori model during the conditioning process to better characterize the real aquifer properties.

The method is applied to two different sets of data, both non-multiGaussian. One is based on a 2D synthetic aquifer and another on a real-complex case study, the Macrodispersion Experiment (MADE-2), site on Columbus Air Force Base in Mississippi (USA). The importance of implementing inversion methods able to yield a posteriori structures is proved to be especially necessary in real case studies where the data assimilation during the inversion procedure may play a major role in both uncertainty reduction and reliability in the model outcomes.

2 Materials and Methods

The GC method constitutes a stochastic inverse modeling technique for the simulation of conductivity (K) fields, which was developed to overcome several of the limitations found in the already existing techniques. The GC method was presented in Capilla and Llopis-Albert (2009), while an exhaustive verification on a 2D synthetic aquifer was shown in Llopis-Albert and Capilla (2009b). A 3D application to the Macrodispersion Experiment (MADE-2) site, on a highly heterogeneous aquifer at Columbus Air Force Base in Mississippi (USA) was presented in Llopis-Albert and Capilla (2009a). The method was extended to deal with fractured rocks (Llopis-Albert and Capilla 2010b) and to take into account independent stochastic structures (Llopis-Albert and Capilla 2010a). Finally, the method was coupled with a hydro-economic modeling framework for dealing with nonpoint agriculture pollution under groundwater parameter uncertainty (Llopis-Albert et al. 2014). For the sake of conciseness, the reader is referred to those papers for all details of the methodology, and only a brief description of the capabilities of the GC method is subsequently presented.

The GC method consists of an iterative optimization process for constraining stochastic simulations to flow and mass transport data. This is performed by means of successive non-linear combinations of seed conditional realizations with the conditional K field resulting from the previous iteration. The a priori stochastic structure of these K seed fields is defined by means of the local cumulative density functions (ccdf's) and the indicator variograms of the log K fields, thus allowing the GC method to adopt any Random Function (RF) model. The consideration of the non-multiGaussian feature allows the reproduction of strings of extreme values of K that often take place in nature and can be crucial in order to obtain realistic and safe estimations of mass transport predictions (e.g., Gómez-Hernández and Wen 1998). The flexibility of this framework allows integrating not only hard data (parameter measurements) but also secondary information (obtained from expert judgement and/or geophysical surveys), transient piezometric or pressure measurements; and concentration and travel time data. Other inverse modelling techniques deal with secondary information incorporating it in initially generated fields to be perturbed, not having any implemented constraint to keep honouring these data. By means of this way of operating, it is possible to generate multiple equally likely K fields (seed fields) conditional to K measurements and secondary information, and to compute the local ccdf at every point or discretization block. Furthermore, the GC method honours the a priori ccdf's during the whole conditioning process. In addition, the GC method is able to deal with different conductivity (K) stochastic structures, belonging to independent K statistical populations (SP) as presented in Llopis-Albert and Capilla (2010a). For instance, SP belonging to fracture families and the rock matrix, each one with its own statistical properties and conditional to their own data. This is carried out by applying independent deformations to each SP during the conditioning process for constraining stochastic simulations to data. Other inverse modeling techniques can be applied to stochastic fields made up by different statistical populations but without honouring the independence of the different stochastic structures.

As a first step, the GC method builds linear sequential combinations of multiGaussian K fields that honour K data and secondary data (Hu 2000):

$$K^m = \alpha_1 K^{m-1} + \alpha_2 K_{2m} + \alpha_3 K_{2m+1} \quad \text{with } K^0 = K_1 \qquad (1)$$

where subscripts stand for seed fields and superscripts for conditional fields resulting from a previous linear combination. That is, at m iteration, the field K^{m-1}, from the previous iteration, is combined with two new independent realizations K^{2m} and K_{2m+1}. The procedure requires combining at least three conditional realizations at a time to ensure the preservation of mean, variance,

variogram and K data in the linearly combined field, for which linear combination coefficients must fulfil several constraints. The coefficients have also to fulfill the constraints in Eq. (2).

$$\begin{cases} \alpha_1 + \alpha_2 + \alpha_3 = 1 \\ (\alpha_1)^2 + (\alpha_2)^2 + (\alpha_3)^2 = 1 \end{cases} \tag{2}$$

being the parameterization of α_i given by Eq. (3):

$$\begin{cases} \alpha_1 = \dfrac{1}{3} + \dfrac{2}{3}cos\theta \\ \alpha_2 = \dfrac{1}{3} + \dfrac{2}{3}sin\left(-\dfrac{\pi}{6} + \theta\right) \text{with } \theta \in [-\pi, \pi] \\ \alpha_3 = \dfrac{1}{3} + \dfrac{2}{3}sin\left(-\dfrac{\pi}{6} - \theta\right) \end{cases} \tag{3}$$

The α_i coefficients are different in every iteration m, and correspond to a unique parameter θ; note the one to one correspondence between the parameter and the combined realization K^m.

Because the linear combination of independent non-Gaussian random functions does not preserve the non-Gaussian distribution, although the variogram is preserved, a transformation between Gaussian to the non-Gaussian fields (and vice versa) is required. This transformation is performed through the probability fields (see Capilla and Llopis-Albert (2009) for more details), which are obtained by sampling the local ccdf's.

Travel time conditioning data may also be considered through a backward-in-time probabilistic model (Neupauer and Wilson 1999), which extends the applications of the method to the characterization of unknown sources of groundwater contamination and to delineate well capture zones. The model is run until a defined maximum number of optimization iterations are reached or a convergence criterion is achieved. By using enough iterations, the procedure converges always to a global minimum due to the mutual independence of the seed fields. Furthermore, it avoids complex parameterizations since the penalty function depends only on one parameter. In addition, because of the implementation of the inverse model, the calibration process is performed with high computational efficiency. The implementation of the method uses a Lagrangian approach, by means of a random walk particle tracking (RWPT), to solve the mass transport equation. This avoids the numerical dispersion usually found in Eulerian approaches. Additionally, a dual-domain approach with a first-order mass transfer approach was implemented to deal with highly heterogeneous and non-Gaussian media, which allows reproducing anomalous breakthrough curves. This is because the dual-domain approach allows taking into account local-scale physical heterogeneity that can lead to transport along preferential pathways, which are difficult or even impossible to reproduce by high-resolution models (see Llopis-Albert and Capilla 2009a).

The particle distribution between the mobile domain and the immobile domain is determined by performing a Bernoulli trial on the appropriate phase transition probabilities.

Finally, at each iteration m of the method the parameter θ is determined by minimizing an objective function that penalizes deviations among computed and measured data. As above explained, this way of operating has been successfully applied in both synthetic and real cases. The penalty function to be minimized is made up by the weighted sum of three terms:

$$p^k(\theta) = p_h^k(\theta) + \Phi^k p_c^k(\theta) + \Psi^k p_\tau^k(\theta) \tag{4}$$

where $p_h^k(\theta)$ is the weighted sum of square differences between observed and calculated values for piezometric heads, concentrations and travel times, respectively. These terms are function

of the parameter θ, for every time step t and measurement location i. The terms Φ^k and Ψ^k are trade-offs coefficients between the different conditioning data.

3 Results and Discussion

3.1 Application to a 2D Synthetic Data Set

The flow domain has a sized of 226.4×246.4 m and is discretized in 37×34 square blocks of size 6.6 m with prescribed head boundary conditions and transient flow conditions with three stress periods of length 31.7, 761 and 2,378.27 years, respectively (Fig. 1). With regard to external stresses, a pumping well with a rate of 1.8 l/s is activated during the second stress period. The hydrological parameters required by the inverse model are defined as follows: porosity of 0.35, longitudinal dispersivity of 0.3 m, transversal dispersivity of 0.03 m, specific storage of $2.5 \ 10^{-4}$ 1/m and a number of 4,900 particles are used to solve the transport equation. The hydraulic conductivity seed fields (only conditioned to K data) have been generated by sequential indicator simulation, using the code ISIM3D (Gómez-Hernández and Srivastava 1990). A variance of the log K equal to 0.5 and a mosaic variography have been defined, which is spherical, with equal ranges in all directions of 40 m, 0.04 of nugget effect, and sill of 0.22. The a priori ccdf displays a highly asymmetrical distribution with a long lower tail, thus assigning higher probabilities of occurrence to high K values. Figure 1 shows additional information about well and initial particle locations. Figure 2 depicts the K reference field, which has been selected between the generated seed fields, and its corresponding frequency distribution and univariate statistics. This figure also presents the same for the first realization of a conditioned field after 50 iterations of the optimization procedure. The simulated fields are conditional to all available data, i.e., conductivity measurements (K), piezometric head measurements (h) and solute concentration measurements (c).

Figure 3 shows the piezometric head fields at the end of the three stress periods defined and the spatial location for the following sets of conditioning data: sixteen regularly spaced K measurements, sixteen regularly spaced h measurements at the end of the three time steps considered and forty c measurements distributed in time and space to capture the shape and extension of the plume. Three snapshots were considered at times 412.22, 792.74 and
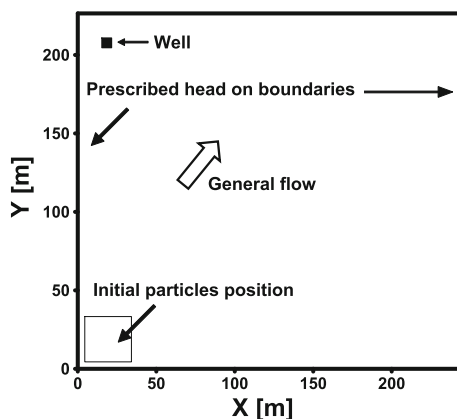

Fig. 1 Geometry, boundary conditions, initial location where particles are released and well position
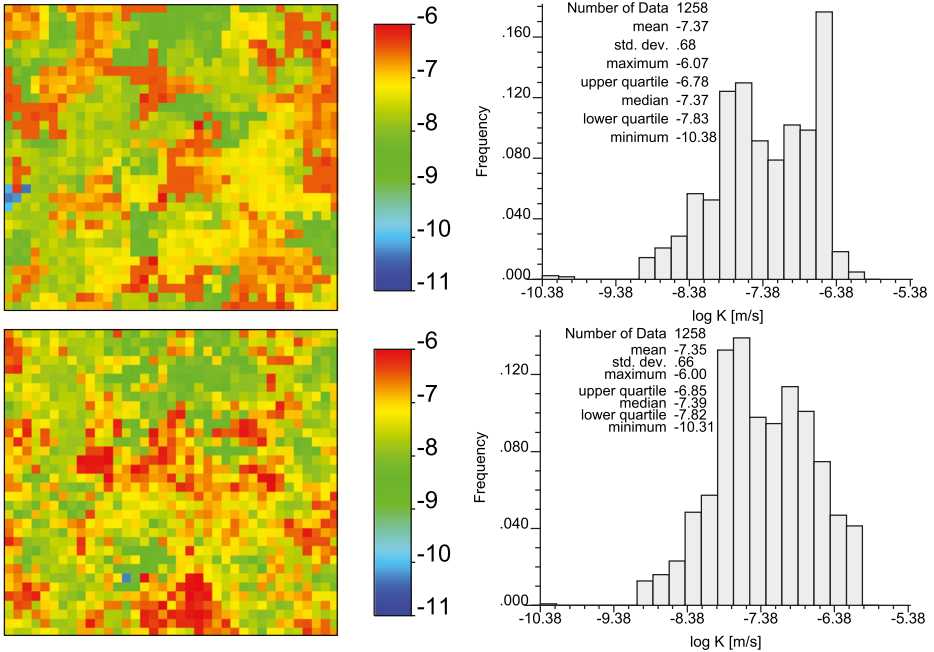
Fig. 2 Log K (m/s) of the reference field and its corresponding frequency distribution and univariate statistics (*above*); and for the first realization of a conditioned field after 50 iterations (*below*)

1,902.58 years. Figure 4 illustrates the probability maps obtained from the local ccdf's, computed from an ensemble of conductivity fields for K seed fields and conditioned fields at iteration 50 of the optimization procedure. A hundred K seed fields were used to obtain the ensemble. The probability maps are presented for the 4 and 6th thresholds (−9.0 and −8.0 log m/s).

Figure 5 presents the indicator variogram maps obtained for the 2nd decile corresponding for the reference log K field and for the first realization of a conditioned field after 50 iterations of the optimization procedure. The indicator variograms are also depict for the average of ensemble seed conductivity fields and conditioned fields, both built by using a hundred realizations.
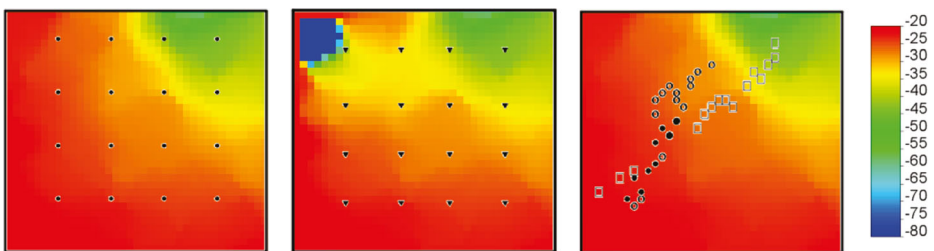

Fig. 3 Piezometric head fields (m) at the end of the three stress periods defined and spatial location for K data, h data at 3 periods and c data at 3 snapshots, t_{c1}=412.22 years (*black dots*), t_{c2}=792.74 years (*white circles*) and t_{c3}=1902.58 years (*squares*) (from left to right)

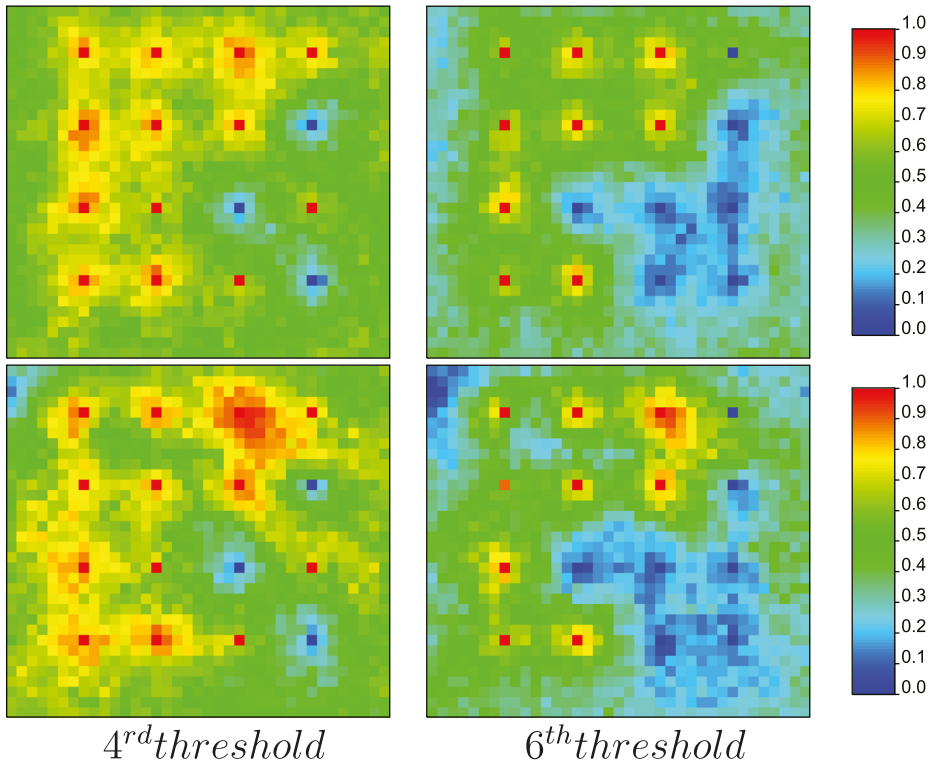$4^{rd} threshold$ $6^{th} threshold$

Fig. 4 Probability maps obtained from the local ccdf's, computed from an ensemble of conductivity fields for K seed fields (*above*) and conditional fields at iteration 50 of the optimization procedure (*below*). The probability maps are presented for the 4th and 6th thresholds (−9.0, and −8.0 log m/s)

The ensemble variograms for K seed fields and conditioned fields illustrate that the method tends to preserve the a priori spatial structure for every threshold, at time that reduces the uncertainty when conditioning to all available information. Furthermore, this is true regardless the iteration number of the optimization procedure or the conditioning information used. Results show the normal ergodic fluctuations for different simulated fields, which disappear at ensemble variograms. This idea is reinforced by the local ccdf's, which display a great similarity for all deciles, leading to a random function model preservation, while the non-multiGaussian feature is also retained (Fig. 4).

Nevertheless, the method can slightly modify the variogram in a certain way to better reproduce the conditioning information and get closer to the unknown reality (see Fig. 2). This can be determined by observing the changes between the K reference field and the conditioned field and also in their corresponding frequency distributions and univariate statistics.

Eventually, probability maps show that the method is able to produce interconnected zones that were not captured by the data used in the a priori stochastic structure, at time that avoid a homogenization of the K field, since the inverse model is able to increase or reduce the K values where necessary. The interconnected zones are reflected in the modified local ccdf's, as shown in Fig. 4.
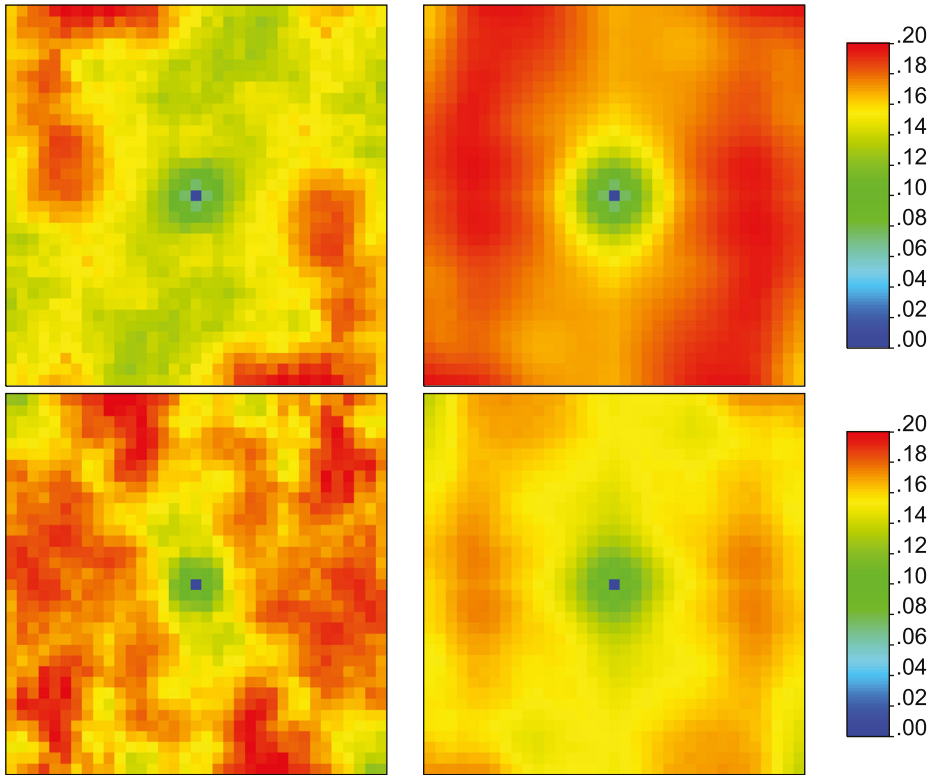
Fig. 5 Indicator variogram maps obtained for the 2nd decile corresponding, from left to right, to the reference log K field and the average of the ensemble seed conductivity fields. Below it is presented the same for the first realization of a conditioned field after 50 iterations of the optimization procedure and the average of the ensemble conditioned conductivity fields

3.2 Application to a 3D Real Case (MADE site)

A large-scale natural-gradient tracer test was conducted in the early '90s in a shallow unconfined alluvial aquifer, which is located on Columbus Air Force Base in northeastern Mississippi. It is commonly referred to as the Macrodispersion Experiment or MADE-2 site. This is a highly heterogeneous aquifer since the natural logarithm of hydraulic conductivity varies several orders of magnitude within a short distance ($\sigma^2_{\ln K} \approx 0.5$).

This project has led to an extensive field database rarely existing in practice and a comprehensive research focusing on different matters such as validating hydrogeochemical and inverse models. There is an exhaustive literature about the MADE-2 experiment. For instance, further information can be found in Boggs et al. (1992), Boggs and Adams (1992), and Adams and Gelhar (1992). The lessons learned from the last 25 years of research at the MADE site was presented in Zheng et al. (2011).

A three-dimensional block centered finite difference grid with a total size of 110 × 280 × 10.5 m was used for modelling the MADE-2 site as a confined aquifer (Fig. 6). The grid spacing is 2 × 2 m in the horizontal direction and 0.5 m in the vertical direction. Constant head conditions along the north and nouth boundaries, and no-flow conditions to the nast and west boundaries, limit the model domain laterally. The spatial location of the conditioning data is
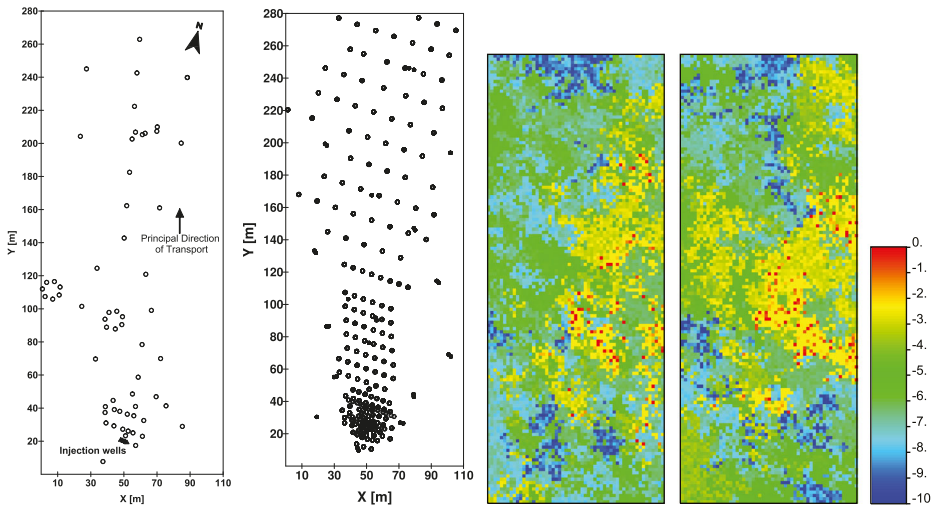
Fig. 6 From left to right: dimensions of the aquifer and spatial location of flowmeter wells and solute injection wells; areal location of head (*black dots*) and concentration (*white circles*) measurements; horizontal slices at $z=$ 3.5 m of hydraulic conductivity (ln K (cm/s)) for a seed field and for a conditioned field

presented in Fig. 6 for the hydraulic conductivity (K), piezometric head (h) and concentration measurements (c). A total of 878 conductivity data, 506 transient piezometric measurements and 1,000 concentration measurements were used as conditional information. Transient flow conditions were considered by defining 15 stress periods with period lengths of a month, thus covering the MADE-2 test duration. Another stress period was added to represent the tritium injection, which was performed through five injection wells for a period of 48.5 h at a uniform rate of 3.3 l × min^{-1} (Fig. 6). A spatial distribution with temporal variations of the recharge was considered.

The GC method was successfully applied to this experiment, as shown in Llopis-Albert and Capilla (2009a). The inverse model obtained a good agreement between data and simulated mass distribution at $t=328$ days, including the non-Gaussian plume behaviour. This work also showed the necessity of using a dual-domain mass transfer approach (or other transport equation different to the advection–dispersion equation) when dealing with upscaled models regardless of what random function is used to generate the K distribution; and the reduction of uncertainty outcomes when conditioning to all available information and not only to K data. The mass transfer rate coefficient for the dual domain approach was 0.0005 day^{-1} with a mobile porosity of 0.043. For the sake of conciseness, the reader may be referred to Llopis-Albert and Capilla (2009a) for further details concerning to the modeling approach.

This work goes a step further by analyzing the changes of the a priori structure when constraining stochastic simulations to data to better reproduce the preferential flow paths (which has an important effect on the anomalous tracer plume spreading at the MADE site) and its impacts on the uncertainty reduction when conditioning to all available information.

The seed hydraulic conductivity fields, which are gradually modified to honour all available data, were generated by sequential indicator simulation using the code ISIM3D (Gómez-Hernández and Srivastava 1990). A geostatistical analysis was performed based on the 2,495 flowmeter measurements of the hydraulic conductivity taken at 62 boreholes (Fig. 6).

The a priori random function modelling is based on a similar indicator geostatistical analysis as presented, for the MADE site by Salamon et al. (2007), although they used a

flowmeter measurement support scale. We assume that depositional structures in the aquifer are approximately horizontal, as sustained by various authors, e.g., Salamon et al. (2007). Hence, spatial continuity is only analyzed in the completely horizontal and vertical direction. No significantly higher spatial continuity in the extreme thresholds was detected in the horizontal plane, in spite of the fact that preferential flow pathways have a significant effect on the anomalous tracer plume spreading at the MADE site, e.g., Zheng et al. (2011). Additionally, other modeller decisions are needed to complete the indicators variography definition because there are not enough K data within each threshold. A higher spatial continuity definition for the extreme thresholds has been adopted, thus allowing the reproduction of existing preferential flow pathways (consistent with results obtained from indicator variography). The iterative optimization process is carried out by combining alternately seed K fields generated with this variography with others without this higher spatial continuity definition. Figure 6 shows horizontal slices at $z=3.5$ m of hydraulic conductivity for a seed and a conditioned field. Figure 7 presents standardized indicator variograms for both seed and conditioned fields for deciles 1 and 5. Once again, it is clear from those figures that the a priori structure is slightly modified according with the additional conditioning information. The modified structure reduces the uncertainty of the model outcomes, which is supported by the good agreement between data and computed values for all conditioned fields (Llopis-Albert and Capilla 2009a). Furthermore, the Monte Carlo simulations, using seed fields, showed the
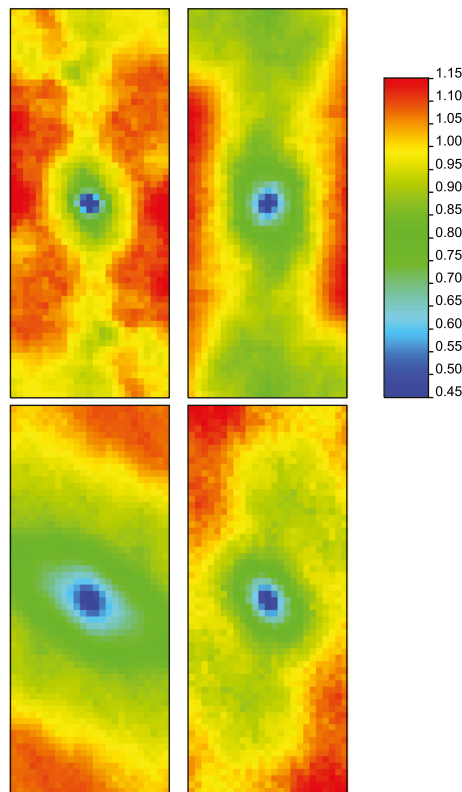

Fig. 7 Standardized indicator variograms for both seed (*left*) and conditioned fields (*right*) for deciles 1 (*above*) and 5 (*below*)

existence of a high uncertainty when not using all available information and the need to condition to as much information as possible. The Monte Carlo technique has been exhaustively used in hydrology to assess uncertainty in the modelling (e.g., Mylopoulos et al. 1999; Abolverdi and Khalili 2010; Zakaria et al. 2012; Charalambous et al. 2013).

As a further research it could be interesting to analyze the change of the a priori RF of the MADE site when using the vertical support scale of flowmeter measurements (15 cm). Note that this work uses a vertical discretization of 0.5 m because of the high computational cost, thus leading to an upscaled model. This may lead to a wrong a priori RF definition after the geostatistical analyses, which should be corrected by the inverse model during the conditioning procedure. When using the vertical support scale of the flowmeter measurements the preferential flows, that play a major role on the anomalous tracer plume spreading at the MADE site (Salamon et al. 2007), could be more accurately characterized. Furthermore, these preferential flows could be treated in the GC method as independent stochastic processes (i.e., different statistical populations) during the whole conditioning process, which represents a great advantage with regard to other inverse models. Then a better agreement between data and simulated mass distribution at time 328 days could be achieved and a lesser change of the a priori RF would be required. This was proved on a fractured rock case study using the GC method (Llopis-Albert and Capilla 2010b), where each fracture plane and the rock matrix were considered as different statistical populations.

4 Conclusions

The GC method tends to preserve the a priori spatial structure of the stochastic process during the iterative optimization procedure of non-linear combinations of K fields, although some modifications can take place to better reproduce the conditioning information and become closer to the unknown reality, at least in terms of honoring other available information. This has been shown in a 2D synthetic case, where the GC method honours the a priori model, which is shared by all seed fields. The a priori model is honoured although showing the normal ergodic fluctuations around it for the different simulated fields. Furthermore, additional conditioning data, that implicitly integrate information not captured by K data, lead to changes in the a priori stochastic model, as shown for example when reproducing interconnected zones, which might provide safer estimations of mass transport predictions. Nevertheless, in the 3D real case study, results show how the a priori structure is modified not obeying just to fluctuations but possibly to the effect of the additional information on K, implicit in piezometric and concentration data. Finally, both 2D and 3D cases retain the non-Gaussian feature in the conditioned fields, since the variogram is kept for all deciles. We conclude that implementing inversion methods able to yield a posteriori structures that incorporate more data might be of great importance in real cases in order to reduce uncertainty and to deal with risk assessment projects. In these sense, the reduction of the uncertainty has been proved for the MADE site when using the GC method and when constraining stochastic simulations to all available data and not only to K data. This has been achieved due to the change of the a priori structure during the conditioning procedure.

References

Abolverdi J, Khalili D (2010) Development of regional rainfall annual maxima for Southwestern Iran by LMoments. Water Resour Manag 24(11):2501–2526

Adams EE, Gelhar LW (1992) Field study of dispersion in a heterogeneous aquifer 2. Spatial moments analysis. Water Resour Res 28(12):3293–3307

Boggs JM, Adams EE (1992) Field study of dispersion in a heterogeneous aquifer. 4. Investigation of adsorption and sampling bias. Water Resour Res 28(12):3325–3336

Boggs JM, Young SC, Beard LM (1992) Field study of dispersion in a heterogeneous aquifer. 1. Overview and site description. Water Resour Res 28(12):3281–3291

Caers J (2007) Comparing the gradual deformation with the probability perturbation method for solving inverse problems. Math Geol 39(1). doi:10.1007/s11004-006-9064-6

Capilla JE, Llopis-Albert C (2009) Gradual conditioning of non-Gaussian transmissivity fields to flow and mass transport data: 1. Theory. J Hydrol 371:66–74

Carrera J, Alcolea A, Medina A, Hidalgo J, Slooten LJ (2005) Inverse problem in hydrogeology. J Hydrogeol 13: 206–222

Charalambous J, Rahman A, Carroll D (2013) Application of Monte Carlo simulation technique to design flood estimation: a case study for North Johnstone River in Queensland, Australia. Water Resour Manag 27:4099–4111. doi:10.1007/s11269-013-0398-9

De Marsily G, Delhomme JP, Coudrain-Ribstein A, Lavenue AM (2000) Four decades of inverse problems in hydrogeology. Geol Soc Am (Special Paper 348)

Doherty J (1994) PEST: Corinda, Australia. Watermark Computing, 122 p

Gómez-Hernández JJ, Srivastava RM (1990) ISIM3D: An ANSI-C three dimensional multiple indicator conditional simulation program. Comput Geosci 16(4):395–440

Gómez-Hernández JJ, Wen XH (1998) To be or not to be multiGaussian? A reflection on stochastic hydrogeology. Adv Water Resour 21(1):47–61

Gómez-Hernández JJ, Sahuquillo A, Capilla JE (1997) Stochastic simulation of transmissivity fields conditional to both transmissivity and piezometric data. 1. Theory. J Hydrol 203:162–174

Hu LY (2000) Gradual deformation and iterative calibration of gaussian-related stochastic models. Math Geol 32(1):87–108

Llopis-Albert C, Capilla JE (2009a) Gradual conditioning of non-gaussian transmissivity fields to flow and mass transport Data: 3. Application to the Macrodispersion experiment (MADE-2) site, on Columbus air force base in Mississippi (USA). J Hydrol 371:75–84

Llopis-Albert C, Capilla JE (2009b) Gradual conditioning of non-Gaussian transmissivity fields to flow and mass transport data: 2. Demonstration on a synthetic aquifer. J Hydrol 371:53–65

Llopis-Albert C, Capilla JE (2010a) Stochastic inverse modeling of hydraulic conductivity fields taking into account independent stochastic structures: a 3D case study. J Hydrol 391:277–288

Llopis-Albert C, Capilla JE (2010b) Stochastic simulation of non-Gaussian 3D conductivity fields in a fractured medium with multiple statistical populations: a case study. J Hydrol Eng 15(7):554–566

Llopis-Albert C., Capilla JE (2011) Change of the a priori stochastic structure in the conditional simulation of transmissivity fields. P.M. Atkinson and C.D. Lloyd (eds.), geoENV VII – Geostatistics for Environmental Applications, Quant Geol Geostat 16. Springer. ISBN: 9048123216

Llopis-Albert C, Palacios-Marqués D, Merigó JM (2014) A coupled stochastic inverse-management framework for dealing with nonpoint agriculture pollution under groundwater parameter uncertainty. J Hydrol 511:10–16. doi:10.1016/j.jhydrol.2014.01.021

McLaughlin D, Townley LR (1996) A reassessment of the groundwater inverse problem. Water Resour Res 32(5):1131–1161

Mylopoulos YA, Theodosiou N, Mylopoulos NA (1999) A stochastic optimization approach in the design of an aquifer remediation under Hydrogeologic uncertainty. Water Resour Manag 13(5):335–351

Neupauer RM, Wilson JL (1999) Adjoint method for obtaining backward-in-time location and travel time probabilities of a conservative groundwater contaminant. Water Resour Res 35(11):3389–3398

Oliver DS, Chen Y (2010) Recent progress on reservoir history matching: a review. Comput Geosci 15(1):185–221

Poeter EP, Hill MC (1998) Documentation of UCODE, a computer code for universal inverse modeling. US Geol Surv Water Resour Investig Rep 98–4080:116

Rehfeldt KR, Boggs JM, Gelhar LW (1992) Field study of dispersion in a heterogeneous aquifer 3. Geostatistical analysis of hydraulic conductivity. Water Resour Res 28(12):3309–3324

Salamon P, Fernández-Garcia D, Gómez-Hernández JJ (2007) Modeling tracer transport at the MADE site: the importance of heterogeneity. Water Resour Res 43:W08404. doi:10.1029/2006WR005522

Vázquez RF, Beven K, Feyen J (2009) GLUE based assessment on the overall predictions of a MIKE SHE application. Water Resour Manag 23:1325–1349. doi:10.1007/s11269-008-9329-6

Yeh WWG (1986) Review of parameter identification procedures in groundwater hydrology: the inverse problem. Water Resour Res 22(2):95–108

Zakaria ZA, Shabri A, Ahmad UN (2012) Regional frequency analysis of extreme rainfalls in the West Coast of Peninsular Malaysia using partial L-Moments. Water Resour Manag 26(15):4417–4433

Zheng C, Bianchi M, Gorelick SM (2011) Lessons learned from 25 years of research at the MADE Site. Groundw 49(5):649–662

Zhou H, Gómez-Hernández JJ, Li L (2014) Inverse methods in hydrogeology: evolution and recent trends. Adv Water Resour 63:22–37. doi:10.1016/j.advwatres.2013.10.014

Zimmerman DA et al (1998) A comparison of seven geostatistically based inverse approaches to estimate transmissivities for modeling advective transport by groundwater flow. Water Resour Res 34(6):1373–1413